

Evidence for scale similarity of internal intermittency in turbulent flows at large Reynolds numbers

By C. W. VAN ATTA

Scripps Institution of Oceanography, University of California, La Jolla

AND T. T. YEH

Argonne National Laboratory, Argonne, Illinois 60439

(Received 20 May 1974 and in revised form 5 February 1975)

Some new measurements and a reassessment of previous data on statistical properties of the breakdown coefficients $q_{r,l}$ in high Reynolds number turbulence show the existence of a range of scale similarity for scales larger than those in the viscous range ($l \geq 36\eta$). The rate of variation of the probability density $p(q_{r,l})$ with changing outer scale l/η decreases as l/η increases, becoming fairly insignificant for the largest values of l/η . Measurements of characteristic functions of the probability densities show a substantial degree of statistical independence for sequential adjoint values of $q_{r,l}$, consistent with the small values of the correlation coefficients for these variables. The data for the moments of $q_{r,l}$ exhibit a behaviour very close to that predicted by the scale-similarity theory when only data for $r \geq 36\eta$ are considered, i.e. data for smaller inner length scales are excluded. The moments and corresponding values of the parameters μ_p are in good agreement with our previous results and with some earlier data of Kholmyansky, but some rather large unresolved differences in the probability densities of $q_{r,l}$ are found on comparing the present data with those of Kholmyansky. The present measurements of breakdown coefficients for $\zeta_1 = \mathcal{U}^{-1}\partial u/\partial t = \partial(\ln \mathcal{U})/\partial t$ and $\zeta_2 = U^{-1}\partial u/\partial t$, the time derivatives of the streamwise velocity and its logarithm measured in the atmospheric boundary layer, resolve some previous questions concerning the sensitivity of the results obtained to the choice of positive variable, varying sampling rates and the values of external parameters.

For low sampling rates, a systematic change in the shape of the probability densities $p(q_{r,l})$ with varying digital sampling rate is found using either ζ_1 or ζ_2 . For sufficiently high sampling rates, the probability densities are independent of the sampling rate; and invariant results are obtained when the sampling rate is at least one-quarter of the Kolmogorov frequency associated with the viscous length scale based on the turbulent dissipation rate. The probability densities $p(q_{r,l})$ measured using either ζ_1 or ζ_2 are very similar to the corresponding spectra of ζ_1 or ζ_2 respectively. Comparison of the mean-square values of ζ_1 and ζ_2 with an extended form of Taylor's hypothesis shows that the variable ζ_1 is not a good approximation to the true spatial derivative $\partial u/\partial x$, and the use of such an approximation can lead to results that are both qualitatively and quantitatively incorrect.

1. Introduction

The transfer of energy from larger- to smaller-scale motions in turbulent flows at large Reynolds number is often thought of as a cascade involving breakdown of motions on one scale into those on a smaller scale. The idea of a cascade breakdown was introduced by Richardson (1920), and development of this idea by Kolmogorov (1941) and Oboukhov (1941) led to the well-known theory of universal similarity and the inertial subrange for isotropic turbulence. Interest in studying the mechanism of this breakdown has increased in connexion with questions about statistical properties of the rate of energy dissipation first raised by Landau & Lifschitz (1959), Kolmogorov (1962) and Oboukhov (1962). Specific mathematical models for the breakdown process have been examined by Novikov & Stewart (1964) and Novikov (1965). Another, comparatively more general, model of the breakdown, leading to certain results hypothesized by Kolmogorov and Oboukhov, including a lognormal probability distribution for the rate of dissipation of energy and related quantities, has been given by Yaglom (1966) and Gurvich & Yaglom (1967). Since then, as discussed, for example, by Van Atta & Yeh (1973), experimental data have accumulated indicating that these models do not correctly describe the behaviour of measurable quantities, and that a theory with fewer specific constraints on the form of the probability densities of averaged and unaveraged dissipation rates and related variables is required.

In an attempt to find more general laws for the structure of internal intermittency in turbulent flows at large Reynolds numbers, Novikov (1969, 1971) proposed a theory of scale similarity which furnished predictions of some of the statistical properties of the breakdown coefficients $q_{r,i}$ defined as the ratios of averages over different spatial regions of positive variables (like the squares of individual velocity derivatives and the local turbulent dissipation rate) characterizing the fine-structure and internal intermittency in high Reynolds number turbulence. Experiments to compare the predictions of scale-similarity theory with internal intermittency in high Reynolds number turbulence have been inconclusive. The initial interpretation of our earlier experimental results (Van Atta & Yeh 1973, hereafter referred to as I) for moments of the breakdown coefficients $q_{r,i}$ strongly questioned the validity of scale similarity, and led to an unsatisfactory rationalization of the observed behaviour of the moments in terms of deviations from scale-similarity behaviour of the probability densities of the $q_{r,i}$. An independent study by Kholmyansky (1973) indicated somewhat closer agreement with scale-similarity predictions, but raised a number of new unanswered questions. The experimental conditions and methods of data analysis in these two studies were quite similar, as were some of the results and conclusions. However, some of the statistical characteristics of the breakdown coefficients chosen for detailed study were quite different and interpretation of the results led to quite diverse conclusions. Kholmyansky's work also suggested important qualitative differences between results obtained for different fine-structure variables and uncovered an essential dependence of the measured probability densities on the sampling rate. Comparison of these two complementary studies

thus revealed a number of open questions regarding the adequacy of methods of data analysis, differences in the results for different fine-structure variables and the sensitivity to variations in external parameters. The present study reassesses and extends the measurements reported in I in order to achieve a more complete comparison with the experimental results reported by Kholmyansky and with the theory of Novikov.

2. Review and discussion of theoretical relations, previous experiments and sampling considerations

2.1. Theory and previous experimental results on scale similarity

Novikov (1971) obtained, under certain assumptions, quite simple universal laws independent of the large scale of the turbulent field which are applicable to the statistical characteristics of the breakdown coefficients. Here, we briefly summarize these results and consider some new experimental questions which have arisen from measurements of various statistical properties of the breakdown coefficients. Similar summaries may be found in Kholmyansky (1973) and in I, so here we emphasize those aspects not previously discussed in both references but which are necessary for the present comparisons.

Novikov considered a non-negative random function $y(x)$ (in our case the square of the time derivative of the streamwise velocity \mathcal{U} or its logarithm) that is statistically homogeneous and isotropic on spatial length scales less than a certain external scale L . A one-dimensional process of this type is investigated for ease of comparison with experimental work, in which it is common practice to measure one-dimensional characteristics of the random field. Novikov singled out three segments in the x direction enclosed in one another with lengths $r < \rho < l$, and considered the ratios of the values of the functions $y(x)$ averaged over these segments. These ratios are called the breakdown coefficients $q_{r,l}$, etc., where

$$q_{r,l}(\bar{h}, x) = y_r(x')/y_l(x) \quad (r < l), \quad (1)$$

$$y_l(x) = \frac{1}{l} \int_{x-\frac{1}{2}l}^{x+\frac{1}{2}l} y(x_1) dx_1, \quad -\frac{1}{2} \leq \bar{h} = \frac{x' - x}{l - r} \leq \frac{1}{2}. \quad (2)$$

The inequality for \bar{h} implies that the smaller segment is included in the larger one. The geometry of the sampling interval is illustrated in figure 1, in which for clarity only two of the sampling lengths, l and r , are shown.

The probability densities of the $q_{r,l}$ for a homogeneous field $y(x)$ depend upon l and r and, in general, upon \bar{h} , since the joint probability density of $y_r(x')$ and $y_l(x)$, and therefore the correlation between these two quantities, may depend on \bar{h} . The moments of the $q_{r,l}$ are defined as

$$a_p(r, l, \bar{h}) \equiv \langle q_{r,l}^p(\bar{h}, x) \rangle. \quad (3)$$

The dependence on \bar{h} (called the 'eccentricity' by Kholmyansky) defines the inhomogeneity of the breakdown. For the square of the streamwise velocity derivative $\partial u/\partial t$, it was found in I that there is a considerable dependence on \bar{h} for the values of the higher moments and a small but clearly defined effect on the value of the lowest moment (mean value). The measured moments are nearly

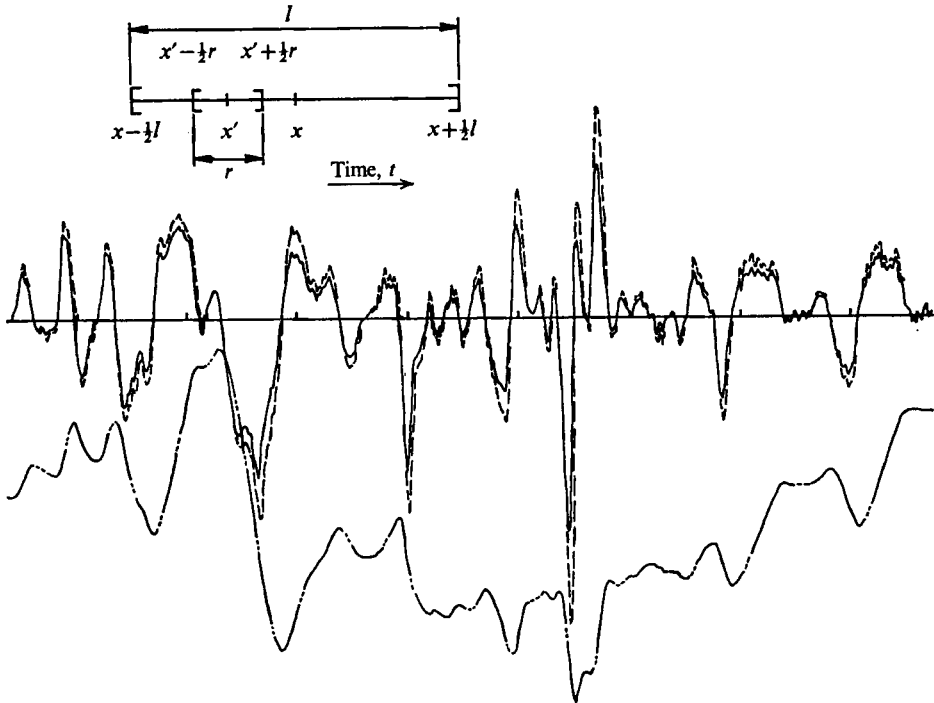


FIGURE 1. Definition of breakdown-coefficient sampling intervals and short sample of data used for calculations. The r shown corresponds to a length of 36η . - - - -, ζ_1 ; —, ζ_2 ; - · - ·, $u(t)$. The interval spacing on the time axis is 0.01 s.

symmetrical functions of the displacement of the shorter segment from the centre of the larger one, with a minimum value when the shorter segment is centrally located within the larger one. Essentially the same result was found by Kholmyansky using the variable $\zeta_1 = \mathcal{U}^{-1} \partial u / \partial t$ instead of $\zeta_2 = U^{-1} \partial u / \partial t$, where $\mathcal{U} = U + u$ is the instantaneous total longitudinal velocity. For $l/r = 2$, he found that the measured probability densities $p(q_{r,l})$ were nearly identical for $h = \pm 0.5$ and that both densities had a larger maximum value and smaller values in the tails of the distribution than that for $h = 0$.

Novikov defined conditions for scale similarity of the $q_{r,l}$ for l and r in the interval of scales for which $L \gg l > r \gg \eta$. Here η is the Kolmogorov microscale $\eta = (\nu^3/\epsilon)^{1/4}$, where ϵ is the average turbulent kinetic energy dissipation rate per unit mass of fluid and ν is the kinematic viscosity. L is a length scale over which gross features of the flow, like the mean velocity in a shear flow, change appreciably. It follows from the definition that self-similarity, if it occurs, is a feature of the inertial subrange. The two conditions for self-similarity are that (i) the probability density of $q_{r,l}$ depends only upon the scale ratio l/r and h , and (ii) two sequential breakdown coefficients $q_{r,\rho}$ and $q_{\rho,l}$ having the same h are statistically independent. From these conditions and (3) it follows that all moments of the breakdown coefficients must have power-law variation with l/r :

$$a_p(l/r, h) = (l/r)^{\mu_p(h)}, \quad (4)$$

where
$$\mu_p(h) - \mu_q(h) \leq p - q, \quad \mu_p(h) \leq p, \quad \mu_0(h) \equiv 0. \quad (5)$$

If the inhomogeneity of breakdown (dependence on h) is suppressed, then

$$\mu_p \leq \mu + p - 2 \quad (p \geq 2), \quad \mu_1 = 0, \quad 0 < \mu_2 \equiv \mu < 1. \quad (6)$$

The characteristic function of the logarithm of the breakdown coefficient is

$$\psi(s, l/r, h) = \langle \exp \{isZ_{r,i}(h, x)\} \rangle, \quad (7)$$

where

$$Z_{r,i}(h, x) = \ln q_{r,i}(h, x)$$

and s is the new variable in the Fourier transform. Novikov showed, assuming scale similarity, that

$$\psi(s, l/r, h) = \psi(s, \rho/r, h) \psi(s, l/\rho, h) \quad (8)$$

and that

$$\psi(s, l/r, h) = (l/r)^{-\alpha(s, h)}, \quad (9)$$

$$\alpha(s, h) = -\ln \psi / \ln (l/r). \quad (10)$$

The universal function $\alpha(s, h)$ is related to the power-law variation of the moments by the expression

$$\mu_p(h) = -\alpha(-ip, h). \quad (11)$$

If the effect of heterogeneity can be neglected, then $\alpha(s)$ is a complex function of s only.

The measurements in I showed that, as the scale ratio l/r changes, the probability density of $q_{r,i}$ evolves from a sharply peaked, negatively skewed density for large values of the scale ratio to a very symmetrical distribution when the scale ratio is equal to two, and then to a highly positively skewed density as the scale ratio approaches one. For fixed l/r , the data clearly showed appreciable systematic variations in the measured probability densities for different values of l/η . The principal features of these systematic changes were a monotonic increase in the peak value and a decrease in the tails of the densities with increasing l/η , which caused a general decrease in the values of the measured moments a_p with increasing l/η over most of the range of possible scale similarity ($L \gg l > \rho > r \gg \eta$). It was therefore concluded that the scale-similarity assumption that the probability density of the breakdown coefficient is a function only of the scale ratio l/r is not satisfied for high Reynolds number turbulence in the atmospheric boundary layer. Measurements to test the degree of independence of adjoint values of $q_{r,i}$ ($q_{r,\rho}$ and $q_{\rho,i}$) were less conclusive. The measured correlation between adjoint values of $q_{r,i}$ was quite small, with the correlation coefficient ranging between +0.04 and +0.12, suggesting a substantial degree of statistical independence, but not incontestably proving this since uncorrelated variables need not be independent. Comparison of moment ratios with those expected for independence showed less agreement as the order of the moment increased.

As a more direct test of independence, Kholmyansky chose to work with the characteristic functions of (8). Defining the product

$$\psi^*(s, l, \rho, r, h) = \psi(s, l, \rho, h) \psi(s, \rho, r, h) \quad (12)$$

he compared the ψ^* computed using measured values on the right-hand side of (12) with the directly measured values of $\psi(s, l, r, h)$. If the variables $q_{r,\rho}$ and $q_{\rho,i}$ are statistically independent, $\psi^* = \psi$. Comparing these relations for four

ratios of the lengths r, ρ and l , he found fairly good agreement for three of the cases but very poor agreement for the fourth. The case for which there was poor agreement involved calculations for $l/r = 32$, and he felt that his calculation of the probability density in this case probably only very roughly represented the true distribution. This was caused by the fact that the density for $l/r = 32$ is sharply peaked and highly skewed (see I), seriously degrading the resolution of his calculation, which used only 64 equally spaced intervals of $q_{r,l}$. These calculations also suffer from the common deficiency of all tests of independence, i.e. one does not know how large a degree of dependence is implied by deviations of a given magnitude from the relation (in this case $\psi^* = \psi$) implied by complete statistical independence.

The logarithm of the breakdown coefficient $q_{r,l}$ is a natural variable to use for tests of independence, since it leads to simple products of characteristic functions of sequential breakdown coefficients $q_{r,\rho}$ and $q_{\rho,l}$. In the present work, we have also used the characteristic function of $q_{r,l}$ itself in tests of independence. In this case, we define the characteristic function of $q_{r,l}$ as

$$\phi(s, l, r, h) = \langle \exp isq_{r,l} \rangle.$$

Then, if $\phi^+(s)$ is the characteristic function of the sum $q_{r,\rho} + q_{\rho,l}$, one can easily show that if $q_{r,\rho}$ and $q_{\rho,l}$ are independent then $\phi(s, l, r, h) = \phi^+(s, h)$, where

$$\phi^+(s, h) = \phi(s, l, \rho, h) \phi(s, \rho, r, h). \quad (13)$$

2.2. Effect of varying the sampling frequency

Because of computer (Minsk-22) memory size limitations, Kholmyansky was unable to perform calculations for the largest scales he desired using his original sample rate of 9500 samples/s. Instead, he obtained such results by using only every fourth point of the sampled data, and this led to two interesting discoveries. First, he found that for the same values of r and l the measured distributions of $q_{r,l}$ were significantly different, the distribution measured with the higher sampling rate having a larger peak value and correspondingly smaller tails. This explicitly raised the important question of what sampling frequency is sufficient for measuring the breakdown coefficient, and whether or not either the previous measurements of I or those of Kholmyansky's study using the higher sampling rate were correct. In both I and Kholmyansky's work, the sampling rate was intuitively chosen to approximate the Kolmogorov frequency $f_K = U/\eta$, i.e. the frequency corresponding to convection at the mean velocity U of the finest-scale variations in the turbulent structure past the probe. Although the Nyquist sampling theorem ensures that this sampling rate is sufficient for obtaining the spectrum of the derivative, one cannot be sure *a priori* that the nonlinear operations (squaring, averaging and then dividing) involved in obtaining $q_{r,l}$ will not lead to a more stringent sampling-rate requirement. One might expect in general that the requirement would differ for the two variables $U^{-1} \partial u / \partial t$ and $\mathcal{U}^{-1} \partial u / \partial t$. As there appears to be no sampling theory available for variables like $q_{r,l}$, an experimental assessment of this point is necessary, and was carried out in the present work.

Kholmyansky also found that for the lowered sampling rate the probability

densities obtained for the two largest values of l were practically the same. This led him to speculate that, if measurements of $p(q_{r,l})$ were made at substantially larger vertical heights above the ground, a range of scale similarity in which the relation $p(q_{r,l}) = p(l/r)$ was closely satisfied, within experimental error, might be found. Such a range was not observed in his data for the larger, sufficiently rapid, sampling rate (associated with smaller values of l) nor in the data of I.

3. Experimental data and analysis

The basic data for the streamwise velocity derivative used in the present measurements were the same as those used in I, and described in some detail there and also by Wyngaard & Pao (1972). Single hot wires, $5\ \mu\text{m}$ in diameter and $1.2\ \text{mm}$ long, were operated in the linearized constant-temperature mode at heights $z = 5.66$ and $11.3\ \text{m}$ above a horizontally homogeneous Kansas prairie. The mean velocity U was $3.78\ \text{m s}^{-1}$ at $z = 5.66\ \text{m}$ and $4.47\ \text{m s}^{-1}$ at $z = 11.3\ \text{m}$. The Kolmogorov microscale η was $0.08\ \text{cm}$ at $z = 5.66\ \text{m}$ and $0.087\ \text{cm}$ at $z = 11.3\ \text{m}$. Streamwise velocity derivatives were obtained by on-line analog filtering. The analog data were played back in the laboratory at the Department of Applied Mechanics and Engineering Sciences, UCSD, and sampled with a 12 bit analog-to-digital converter at a sample rate of 4172 samples/s. The digital data were then processed at UCSD with a CDC 3600 computer. Since only the velocity derivative and not the velocity itself was available on the analog tape, the total velocity \mathcal{U} , which was necessary for the calculations using ζ_1 , was calculated from the derivative signal by numerical integration, which consisted simply of summation of the closely spaced sampled data for the derivative. The resulting time history of ζ_1 is qualitatively similar to that of ζ_2 , as illustrated in figure 1, the values of $\partial u/\partial t$ being modulated with the local values of $\mathcal{U}^{-1}(t)$. As a further check on the accuracy of the numerical integration, the spectrum of $u(t)$ was computed using a standard fast Fourier transform calculation, with the result shown in figure 2. As expected for atmospheric boundary-layer turbulence, for about three decades in energy the spectrum varies nearly like $f^{-5/3}$, and a viscous cut-off occurs at a frequency sufficiently high to indicate that no significant amount of information has been lost in the calculations necessary to compute $u(t)$ in the present indirect fashion.

The digital data for ζ_1 and ζ_2 were squared and averaged over the appropriate number and group of samples corresponding to various values of l , ρ and r , then these averages were used to calculate the values of $q_{r,l}$. The breakdown coefficients are independent of the calibration constants relating the digital data to u and $\partial u/\partial t$. The new time series for the $q_{r,l}$ were then used to compute the probability densities $p(q_{r,l})$, the characteristic functions of $p(q_{r,l})$ (via the numerical Fourier transforms of $p(q_{r,l})$), the moments $a_p(l/r)$ and other statistical quantities. Final results were based on 819 200 data samples, except for the largest averaging lengths ($l/\eta \geq 2320$), for which twice this number of samples was used. The longest time series of data used thus corresponded to about 6.55 min in real time.

Kholmyansky used 5 min records of ζ_1 and ζ_2 . His measurements were made in a clear field on a level section of the Zemlyansk steppe at a height of 13.5 m with a

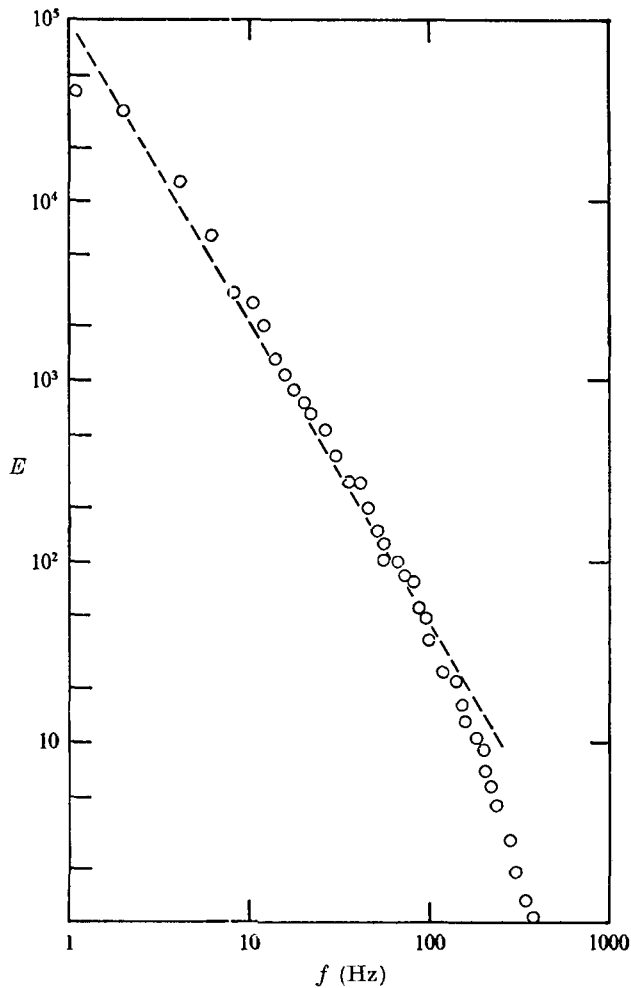


FIGURE 2. Energy spectrum E of $u(t)$ obtained by numerical integration of sampled data for $\partial u/\partial t$. The dashed line has a slope of $-\frac{5}{3}$. Scale of E is relative (uncalibrated) energy per hertz.

mean velocity U of 5.7 m/s. To obtain ζ_1 , the output voltage signal from his constant-temperature hot-wire amplifier went to the input of a nonlinear circuit whose output was proportional to the logarithm of u , and was then differentiated. The data were digitized on-line with a sampling rate of 9500 s^{-1} and later analysed with a Minsk-22 computer. More detailed descriptions of the measurements and analysis have been given by Kholmyansky (1972, 1973).

4. Experimental results

4.1. Effect of sampling rate and choice of fine-structure variable

In order to determine whether our previous calculations (I) had been performed using data sampled sufficiently fast, calculations of $p(q_r, t)$ were performed for four lower sampling rates, and examples of the results are compared in figure 3.

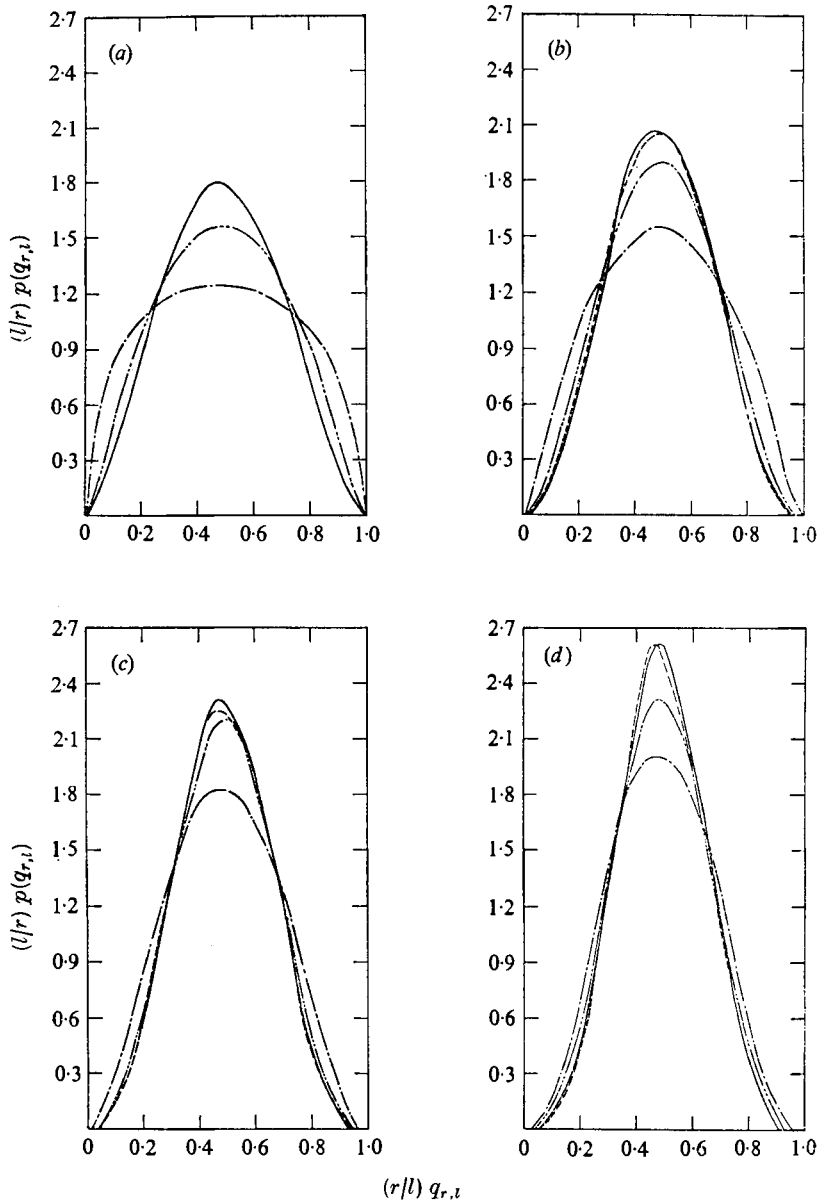


FIGURE 3. Comparison of the measured probability densities $p(q_{r,i})$ of the breakdown coefficient for different sampling rates. $l/r = 2$. Sampling rate, f_s (s^{-1}): —, 4172; ---, 4172/4; - · - ·, 4172/8; — — —, 4172/16. (a) $l/\eta = 145$. (b) $l/\eta = 290$. (c) $l/\eta = 580$. (d) $l/\eta = 1160$. Here and in figures 4–11, all data are for $z = 5.66$ m, $U = 3.78$ ms^{-1} and $h = 0$.

The sampling rate was varied for the present data by using only every fourth, eighth or sixteenth point of the original digital time series of ζ_1 or ζ_2 . The variation in the measured peak values of $p(q_{r,i})$ with the sampling rate is shown in figure 4. The two highest sampling rates produce virtually identical probability densities for all the cases considered, indicating that the calculations reported in I are

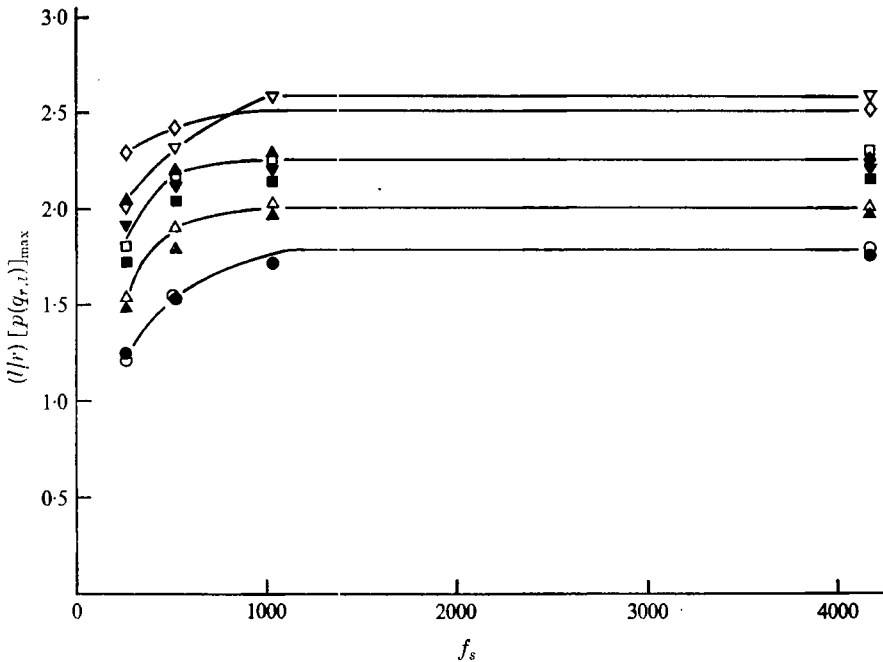


FIGURE 4. Variation of the peak value of $p(q_{r,t})$ with the sampling rate. $l/r = 2$. Open symbols, data for ζ_2 ; solid symbols, data for ζ_1 . \circ , $l/\eta = 145$; \triangle , $l/\eta = 290$; \square , $l/\eta = 580$; ∇ , $l/\eta = 1160$; \diamond , $l/\eta = 2320$.

correct. However, for lower sampling rates, there is a large dependence of the measured probability densities on the sampling rate. As the sampling rate decreases, the peak value decreases and the tails become wider, in agreement with Kholmyansky's results. For both variables, correct results are obtained if the sampling rate is at least 10^3 s^{-1} , or $f_s/f_K \simeq \frac{1}{4}$.

As may be noted from figure 4, the present data produce densities $p(q_{r,t})$ for the smaller values of l/η for the two variables ζ_1 and ζ_2 respectively that are almost the same. For example, for $l/r = 2$ the measured $p(q_{r,t})$ for ζ_1 for $l/\eta = 36.2$, 72.5 and 145 are virtually identical with those reported for ζ_2 in figure 6 of I. However, for larger values of l/η we obtain the results shown in figure 5. The peak value increases more slowly with increasing l/η , and the probability density changes very little for $580 \leq l/\eta \leq 2320$, indicating a range of near scale similarity for the largest values of l/η . This behaviour is qualitatively the same as that found by Kholmyansky for large l/η . He could not express complete confidence in his results as they were obtained with a sampling rate reduced by a factor of four from the original value, corresponding to $f_s/f_K \simeq 0.32$. From figure 4 we should expect this rate to be sufficiently high to furnish correct results, and Kholmyansky's resulting conjecture concerning the possibility of scale similarity for large l/η is supported by the present results. However, the large (30%) discontinuity in Kholmyansky's peak-value data on going from the normal to the reduced sampling rate for $l/\eta \simeq 1617$ is a very disturbing, unexplained discrepancy, whose resolution might alter the previous conclusions. From figures 4 and

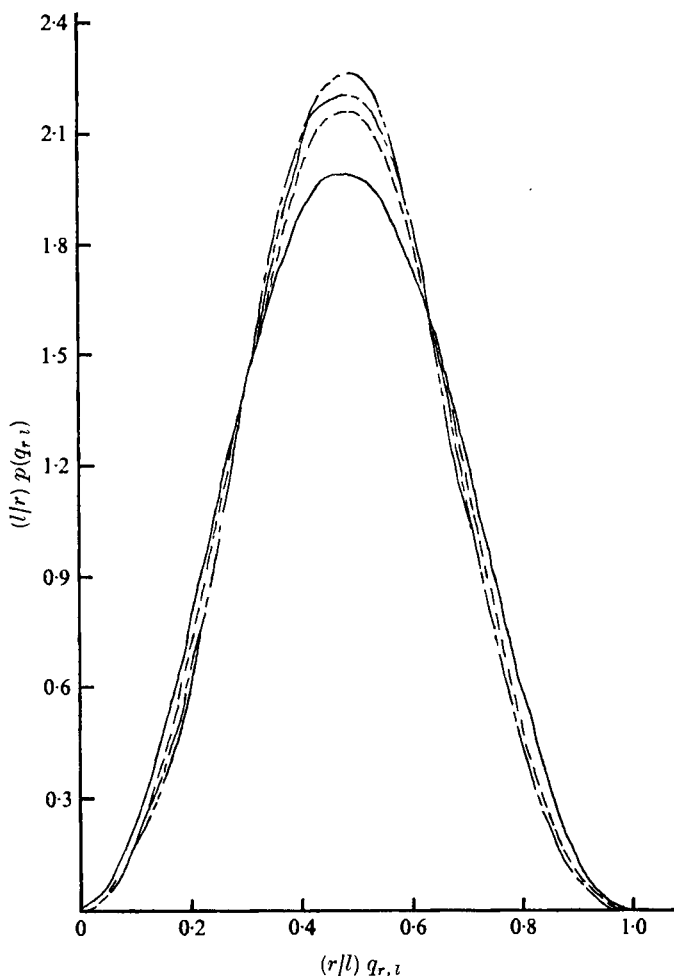


FIGURE 5. Illustrating the near invariance of $p(q_{r,i})$ for large values of l/η , using the variable ζ_1 . $l/r = 2$. —, $l/\eta = 290$; - - -, $l/\eta = 580$; — — —, $l/\eta = 1160$; — · — ·, $l/\eta = 2320$.

6, we note that no such discrepancies were found for the present data. Calculations using the variable ζ_2 for larger values of l indicated that $p(q_{r,i})$ in this case also shows a tendency towards invariance, but this occurs only for scales that are roughly twice as large as those for correspondingly small variations using ζ_1 . This is reflected in the data for $l/\eta = 2320$ in figure 4, which actually show a smaller peak value than the data for $l/\eta = 1160$. As discussed in §4.3, measurements were not pursued in great detail for larger values of l/η , as for these values the length l is becoming as large as the external scale L .

Comparing the peak values of $p(q_{r,i})$ for ζ_1 with those obtained by Kholmyansky reveals another major difference in the two sets of results. As illustrated in figure 6, for $l/r = 2$, the peak values obtained by Kholmyansky are about 50% larger than ours, indicating that his measured probability densities are more sharply peaked. This difference is not due to an insufficiently high sampling rate,

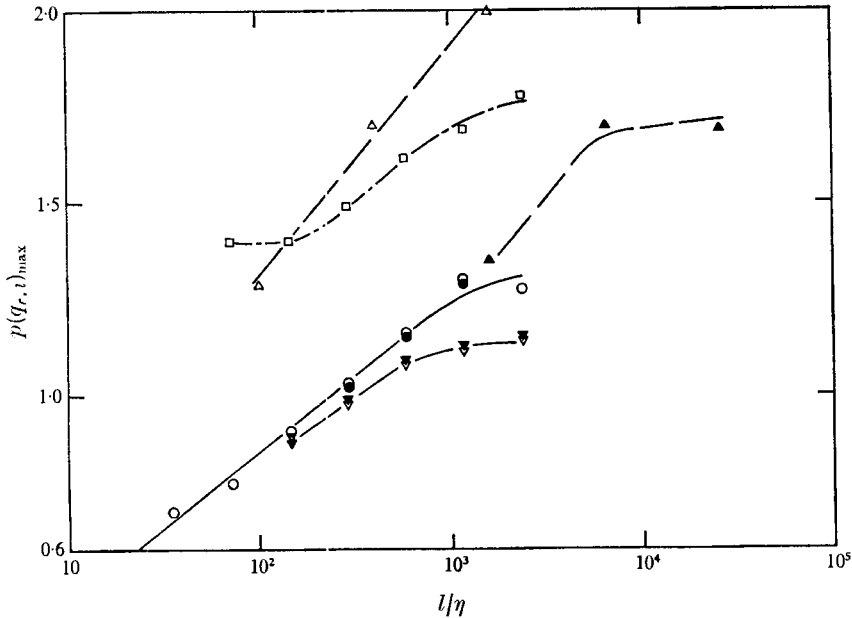


FIGURE 6. Comparison of the variation of the peak value of $p(q_r, l)$ with the outer length l for the present data and those of Kholmyansky. Present data: ∇ , ζ_1 , $l/r = 2$, $f_s = 4172 \text{ s}^{-1}$; \circ , ζ_2 , $l/r = 2$, $f_s = 4172 \text{ s}^{-1}$; \blacktriangledown , ζ_1 , $l/r = 2$, $f_s = 1043 \text{ s}^{-1}$; \bullet , ζ_2 , $l/r = 2$, $f_s = 1043 \text{ s}^{-1}$; \square , ζ_2 , $l/r = 4$, $f_s = 4172 \text{ s}^{-1}$. Kholmyansky: \triangle , ζ_1 , $l/r = 2$, $f_s = 9500 \text{ s}^{-1}$; \blacktriangle , ζ_1 , $l/r = 2$, $f_s = 2375 \text{ s}^{-1}$.

and we have no explanation for it at present. We have not been able to find any stray factor of two which might reconcile the results. The difference may be related to other differences found in the measured spectra of ζ_1 and ζ_2 . Kholmyansky (1972, figure 4) found that, in the inertial subrange, the ratio of the value of the spectrum of ζ_1 to that of the spectrum of ζ_2 was $1.0/0.66$, i.e. the spectrum of ζ_1 was 50% larger. The corresponding ratio $\langle \zeta_1^2 \rangle / \langle \zeta_2^2 \rangle$ of the variances was 1.82. For the present data the same qualitative behaviour is found, as shown in figure 7, but the spectrum of ζ_1 is only about 20% larger than that of ζ_2 in the inertial interval and the ratio $\langle \zeta_1^2 \rangle / \langle \zeta_2^2 \rangle$ is 1.24. Part of the relatively larger difference in Kholmyansky's values for $\langle \zeta_1^2 \rangle$ and $\langle \zeta_2^2 \rangle$ may be due to the fact that his measurements of ζ_1 and ζ_2 were, in fact, not simultaneous, but separated by about 20 min (M. Z. Kholmyansky, private communication). These results indicate that the quantity $\mathcal{U}^{-1} \partial u / \partial t$ is not a close approximation to the local spatial derivative $\partial u / \partial x$. By assuming that velocities and velocity derivatives are uncorrelated and that the various velocity derivatives are related as in isotropic turbulence, Heskestad (1965) found that for large Reynolds numbers

$$\langle \zeta_2^2 \rangle = \langle (\partial u / \partial t)^2 / U^2 \rangle = \langle (\partial u / \partial x)^2 \rangle (1 + \langle u^2 \rangle / U^2 + 2 \langle v^2 \rangle / U^2 + 2 \langle w^2 \rangle / U^2). \quad (14)$$

According to (14), $\langle \zeta_2^2 \rangle$ must be larger than $\langle (\partial u / \partial x)^2 \rangle$. The measurements show that $\langle \zeta_1^2 \rangle$ is even greater than $\langle \zeta_2^2 \rangle$, so we infer that $U^{-1} \partial u / \partial t$ is a better local approximation to $\partial u / \partial x$ than is $\mathcal{U}^{-1} \partial u / \partial t$. It is therefore incorrect, in principle, to

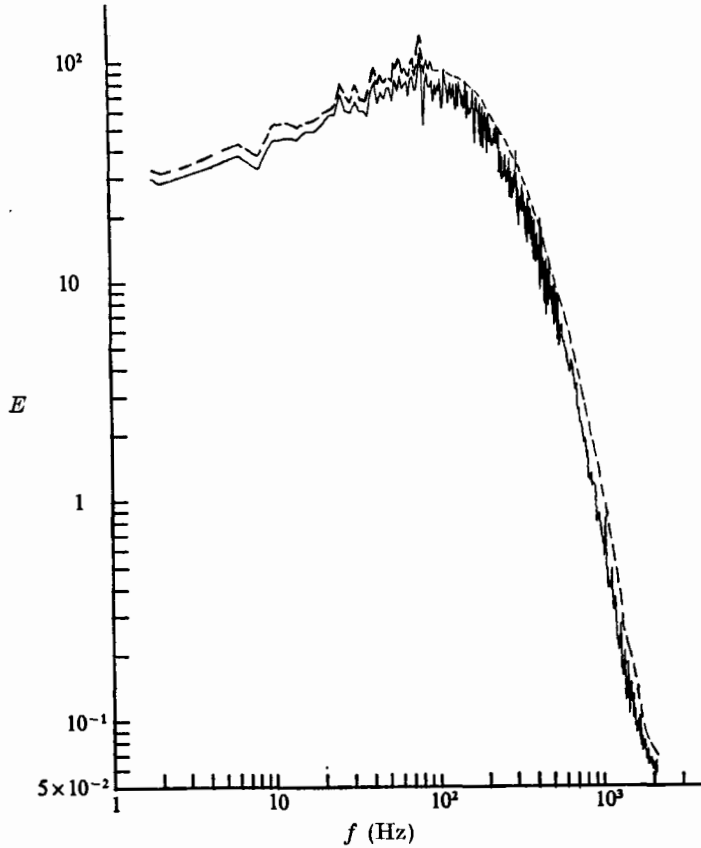


FIGURE 7. Comparison of relative energy spectra for the variables ζ_1 and ζ_2 . —, spectrum of ζ_1 , computer plot; ----, spectrum of ζ_2 , faired through data for $f > 100$ Hz for clarity.

determine the value of ϵ by taking $\partial u/\partial x \approx \mathcal{U}^{-1} \partial u/\partial t$ in the isotropic relation $\epsilon = 15\nu \langle (\partial u/\partial x)^2 \rangle$, as was done by Kholmyansky for comparison with the usual estimate made using ζ_2 . In view of the preceding discrepancy, use of ζ_1 will greatly overestimate the value of ϵ , by a factor of 1.82 in Kholmyansky's case and by a factor of 1.24 for the present data, compared with the customary method using ζ_1 . It would appear that any shortcomings of the usual technique due to corrections to Taylor's original hypothesis (that $\partial u/\partial t = -U \partial u/\partial x$) are much less severe than the error made if one attempts to use ζ_1 to estimate the dissipation rate.

The difference between $\langle (\mathcal{U}^{-1} \partial u/\partial t)^2 \rangle$ and $\langle (U^{-1} \partial u/\partial t)^2 \rangle$ has recently been analysed in detail by J. Park (private communication) for simultaneous \mathcal{U} and $\partial u/\partial t$ measurements obtained in the atmospheric boundary layer at a height of 4.8 m over the ocean with $U = 5.4$ m/s. For $u/U \ll 1$,

$$\zeta_1 = (U + u)^{-1} \partial u/\partial t = (1 - u/U + (u/U)^2 + \dots) \zeta_2, \tag{15}$$

so that

$$\langle \zeta_1^2 \rangle / \langle \zeta_2^2 \rangle = 1 - 2\delta_1 \langle u^2 \rangle^{1/2} / U + 3\delta_2 \langle u^2 \rangle^{1/2} / U^2 - 4\delta_3 \langle u^2 \rangle^{1/2} / U^3 + \dots, \tag{16}$$

$$\text{where } \left. \begin{aligned} \delta_1 &= \langle u \zeta_2^2 \rangle / \langle u^2 \rangle^{\frac{1}{2}} \langle \zeta_2^2 \rangle^{\frac{1}{2}}, & \delta_2 &= \langle u^2 \zeta_2^2 \rangle / \langle u^2 \rangle \langle \zeta_2^2 \rangle, \\ \delta_3 &= \langle u^3 \zeta_2^2 \rangle / \langle u^2 \rangle^{\frac{3}{2}} \langle \zeta_2^2 \rangle. \end{aligned} \right\} \quad (17)$$

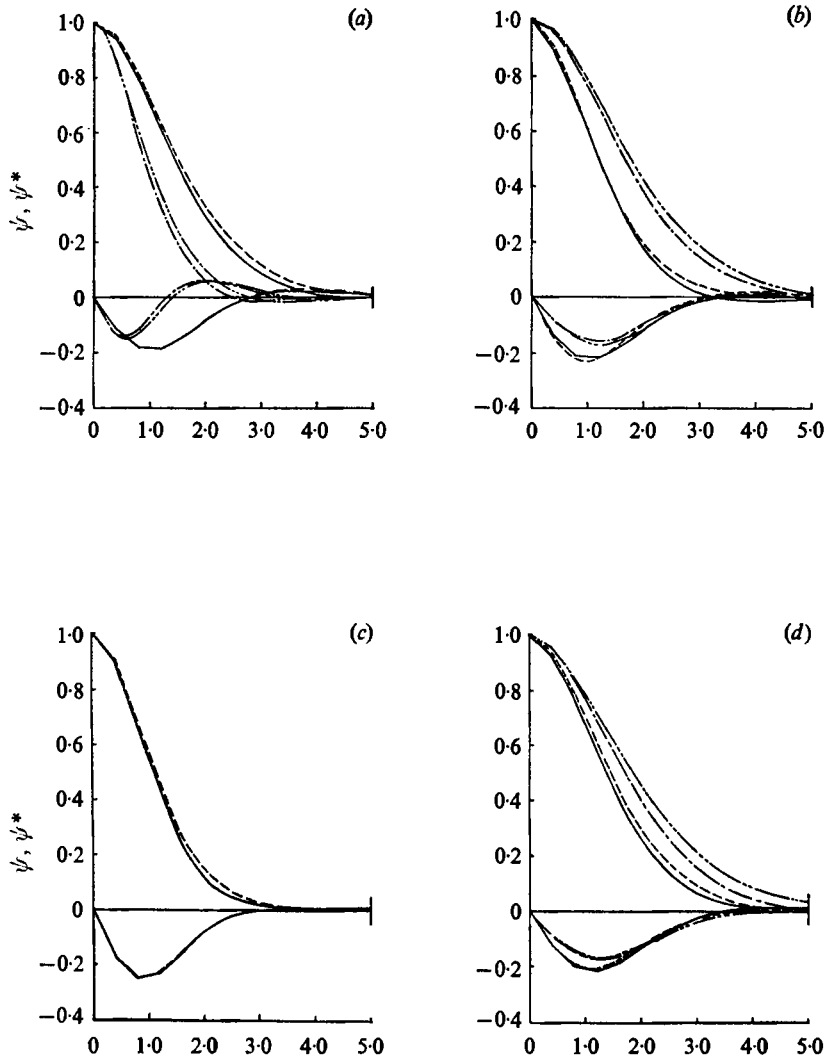
For Park's data, $\delta_1 = -0.113$, $\delta_2 = 1.06$, $\delta_3 = -0.618$, $\langle u^2 \rangle^{\frac{1}{2}}/U = 0.109$ and $\langle \zeta_1^2 \rangle / \langle \zeta_2^2 \rangle = 1.07$. Each of the correlations makes a positive contribution to the right-hand side of (16), and the sum of the three terms accounts for almost all (within 0.5%) of the measured difference between $\langle \zeta_1^2 \rangle$ and $\langle \zeta_2^2 \rangle$. Using Park's δ values to estimate $\langle \zeta_1^2 \rangle / \langle \zeta_2^2 \rangle$ for the present data gives a value of 1.12, which accounts for half of the observed difference. No estimate is possible for Kholmyansky's data, as $\langle u^2 \rangle^{\frac{1}{2}}/U$ was not measured. This analysis provides an explanation for the sense of the differences in the measured values of $\langle \zeta_1^2 \rangle$ and $\langle \zeta_2^2 \rangle$ in different flows and indicates that variations in $\langle \zeta_1^2 \rangle / \langle \zeta_2^2 \rangle$ may be due to a dependence of the δ correlations on experimental conditions. We note that δ_2 will probably always be close to the value of 1.0 that would be expected if the large- and small-scale contributions of the turbulence were independent in the sense assumed in Heskestad's derivation of (14). The same assumption would predict that both δ_1 and δ_3 are zero. The correlation δ_1 , which enters Heskestad's derivation, is indeed fairly small (-0.1), but δ_3 , which is not involved in the derivation, is large (-0.62). These results suggest that experimental comparison of some of the other terms neglected in Heskestad's work might be fruitful.

4.2. Characteristic functions and tests for independence

Comparisons of the computed values of the characteristic functions ψ^* and ψ are shown in figure 8. Both the real and imaginary parts of ψ^* and ψ have the same general shape and appearance, the imaginary part showing somewhat better agreement with the relation $\psi^* = \psi$, which is valid for complete independence of $q_{r,\rho}$ and $q_{\rho,l}$. The real part of ψ^* is consistently larger than that of ψ (except at the origin, where they are both by definition equal to one), and this difference is not a sensitive function of l , ρ or r . For the real part, the agreement with $\psi^* = \psi$ is about the same as that observed by Kholmyansky, while the agreement for the imaginary part is generally closer for the present data. The present characteristic functions, which were calculated from the same data as was used to calculate the probability densities already reported in I, satisfy the consequences of the assumption of independence of $q_{r,\rho}$ and $q_{\rho,l}$ fairly well, with the reservation made above concerning the systematic behaviour of the real part of ψ . The measurements of ϕ and ϕ^+ also show fairly good agreement with the assumptions of independence, as illustrated in figure 9. These results are consistent with the small measured values of the cross-correlation coefficient R for the variables $q_{r,\rho}$ and $q_{\rho,l}$:

$$R = \langle (q_{r,\rho} - \langle q_{r,\rho} \rangle) (q_{\rho,l} - \langle q_{\rho,l} \rangle) \rangle / \langle (q_{r,\rho} - \langle q_{r,\rho} \rangle)^2 \rangle^{\frac{1}{2}} \langle (q_{\rho,l} - \langle q_{\rho,l} \rangle)^2 \rangle^{\frac{1}{2}},$$

which in I was found to range from $+0.04$ to about $+0.12$. As suggested in I, it is quite possible that the observed small systematic deviations from the hypothetical behaviour required by independence can be magnified to produce significant deviations from scale similarity in the higher-order moments. However, with the present evidence regarding independence, it appears likely that



8

FIGURE 8. Characteristic functions of $\ln q_{r,l}$. Of the closely spaced pairs of curves, the solid line or the one with fewer dashes is ψ^* ; the other is ψ . The real parts all begin at the point $(0, 1)$, the imaginary parts at the point $(0, 0)$. (a) ---, $l = 580\eta$, $\rho = 290\eta$, $r = 72\eta$; - - - - , $l = 290\eta$, $\rho = 145\eta$, $r = 72\eta$. (b) - - - - , $l = 4639\eta$, $\rho = 1160\eta$, $r = 145\eta$; - - - - , $l = 4639\eta$, $\rho = 1160\eta$, $r = 145\eta$. (c) - - - - , $l = 2609\eta$, $\rho = 435\eta$, $r = 72\eta$. (d) - - - - , $l = 4639\eta$, $\rho = 580\eta$, $r = 290\eta$; - - - - , $l = 4639\eta$, $\rho = 1160\eta$, $r = 580\eta$.

deviations in the observed behaviour of lower-order moments from that predicted by scale similarity will be caused not by lack of independence but primarily by gross violation of the first hypothesis of scale similarity (i.e. $p(q_{r,l}) \neq p(l/r)$) as observed in I for the smaller values of l/η .

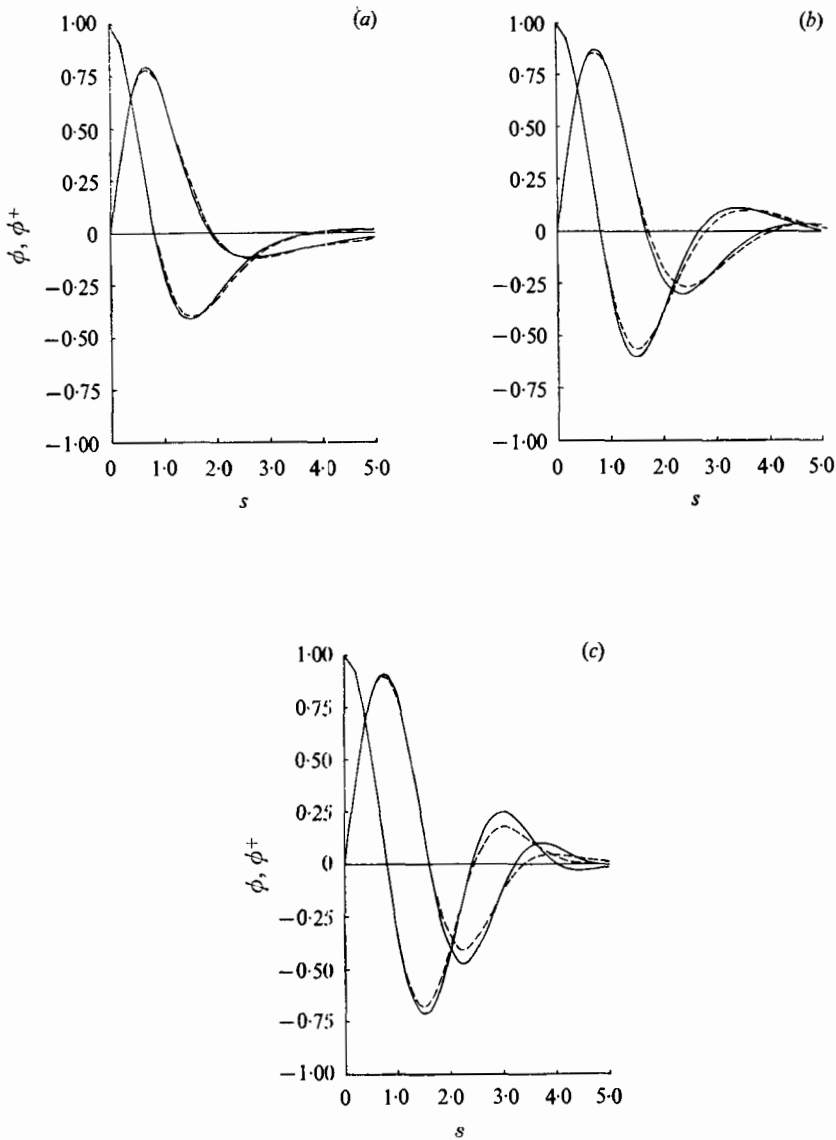


FIGURE 9. Characteristic functions of $p(q_{r,l})$ and $p(q_{r,\rho} + q_{\rho,l})$. —, $\phi^+(s)$; ---, $\phi(s, l, r)$. (a) $l = 2609\eta$, $\rho = 435\eta$, $r = 72\eta$. (b) $l = 580\eta$, $\rho = 290\eta$, $r = 72\eta$. (c) $l = 290\eta$, $\rho = 145\eta$, $r = 72\eta$.

4.3. Moments of $q_{r,l}$

According to (4), if both hypotheses of scale similarity were satisfied, the moments of $q_{r,l}$ would be simple power-law functions of the variable l/r . While the condition of independence of two sequential values of $q_{r,l}$ is fairly well satisfied, the hypothesis that the probability density depends only upon the scale ratio l/r is not satisfied, as found in I. We should not then generally expect to find that the moments a_p of $q_{r,l}$ obey the simple relations which are a consequence of full

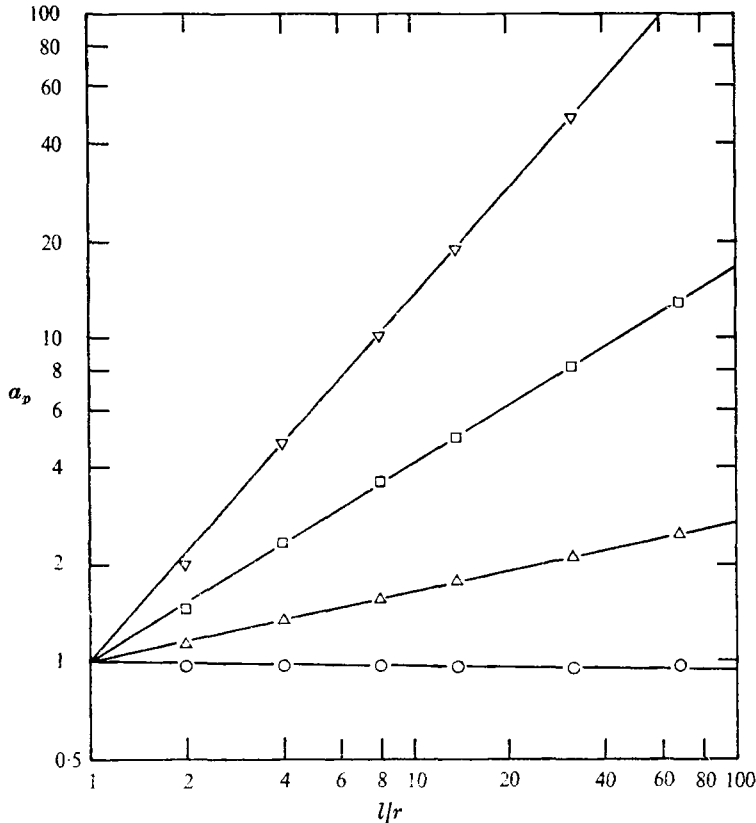


FIGURE 10. Moments of $q_{r,l}$ vs. l/r for fixed value of $r = 36\eta$, using ζ_2 . ○, a_1 ; △, a_2 ; □, a_3 ; ▽, a_4 . Lines through data have slopes μ_p given in §4.3.

scale similarity. In I, the measured moments up to fourth order (using ζ_2 and $h = 0$) were plotted vs. l/r for fixed values of l/η . In many cases these moments are not the simple power-law functions of l/r required by scale similarity, and they do not pass through the point $a_p = 1, l/r = 1$ as required. However, in some cases the moments behave nearly as $(l/r)^{\mu_p}$, and it may be noted that as l/η increases, the moments tend to satisfy relation (4) more closely. For the largest values of l/η (4640 and 5040), the agreement is, in fact, quite good.

Kholmyansky measured the moments of $q_{r,l}$ up to sixth order (using ζ_1), but chose to plot his results vs. l/r for fixed values of r , i.e. he kept the smaller scale fixed and varied l/r by taking l equal to increasing multiples of r . His value of r was 50.5η , while l/η ranged from 101 to 1616, with l/r equal to powers of 2 from 2 to 32, as in I. Kholmyansky's results for the moments (for $h = 0$) up to fourth order show fair agreement with the form predicted for scale similarity, although a good deal of curvature is evident in his plots of $\ln a_p$ vs. $\ln l/r$, and there are systematic deviations from the required limit of $a_p = 1$ at $l/r = 1$ which lie on the high side of the value unity, instead of the low side as for some of the data in I. This observation prompted us to extend our previous computations for the a_p and to replot our previous data for the measured moments keeping r fixed,

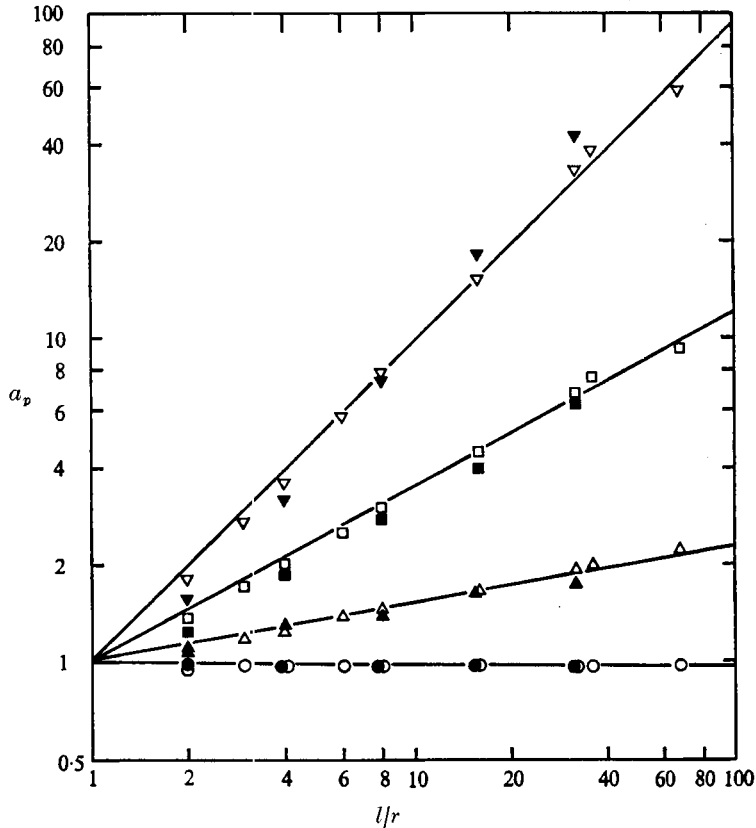


FIGURE 11. Moments of $q_{r,1}$ vs. l/r . Open symbols, present data for ζ_2 , $r = 72.5\eta = \text{constant}$; solid symbols, Kholmyansky data for ζ_1 , $r = 50.5\eta = \text{constant}$. \circ , a_1 ; \triangle , a_2 ; \square , a_3 ; ∇ , a_4 .

instead of keeping l fixed as in I, with the surprising results shown in figures 10 and 11. The measured moments, when plotted in this way, satisfy the relation (4) very closely. The plots of a_p vs. l/r are closely fitted by power laws which pass through the point $a_p = 1$, $l/r = 1$. In figure 11, our data for $r/\eta = 72.4$ (where r corresponds to a length of 64 samples) are compared with Kholmyansky's data for $r/\eta = 50.5$, for which r also corresponded to 64 sampled points. His data for ζ_1 and ours for ζ_2 are in fairly close agreement, and the values of μ_p which one would measure from each are virtually identical. The lowest-order moments are not very sensitive to the differences in the $p(q_{r,1})$ between our data and those of Kholmyansky noted in §4.1, although it is evident from figures 10 and 11 that differences in the moments increase with the order of the moment, as expected. The values of μ_p corresponding to the fitted lines in figure 10 are $\mu_2 = 0.22$, $\mu_3 = 0.61$ and $\mu_4 = 1.13$, and for figure 11 they are $\mu_2 = 0.18$, $\mu_3 = 0.54$ and $\mu_4 = 0.99$. The former are in excellent agreement with the results of Kholmyansky, who found $\mu_2 = 0.19$, $\mu_3 = 0.6$ and $\mu_4 = 1.13$. These results are all quite close to the values previously reported in I, but the present values may be considered more reliable, since they were determined from data which are more closely

of the form expected from (4). We conclude that, as far as the moments a_p and the resulting exponents μ_p are concerned, the results are independent of whether one chooses to work with the variable ζ_1 or with the variable ζ_2 .

The striking agreement of the data in figures 10 and 11 with the form expected for scale similarity confronts us with an apparent paradox, whose resolution lends some insight into the analysis. We must attempt to explain why the same data, when plotted *vs.* l/r in two different ways, in one case (with l/η held constant) show only fair or poor agreement with scale similarity and in the other case (with r/η held constant) show rather remarkably good agreement. Also, if the latter case is representative of true scale similarity, we also have to explain how this can be realized even though the probability densities are not unique functions of l/r only, as required by the underlying hypotheses.

One can rationalize how the data points are mapped in the above fashion by a careful examination of the data presented in I, taking into account that the mapping annihilates some points and is not one-to-one; not all the points from one presentation can be used in the other. This arises because of the restrictions on the fixed values of l or r . Referring to figure 14 of I, we find that, from the plots for l/η held fixed at either 72.5 or 145, only those points for which $l/r = 2$ can be used in our present figure 10 or 11, or only 20% of the original points. For $l/\eta = 290$ and 580, only points for which $l/r = 4, 8$ or 16 may be used in either figure 10 or 11. This trend continues, with values for larger values of l/r being drawn from the old population into the new as l/η increases. Since the measured moments are evolving towards the form predicted by (4) as l/η increases, this selective process effectively screens out those points with large l/r , for which the deviations from scale-similarity behaviour are the largest and are increasing for increasing l/r . When the corresponding points are omitted from figure 14 of I, the remaining points more closely satisfy the self-similar form, but in some cases the number of points remaining is not sufficient to obtain a good estimate. We note that in the plots for the largest values of l/η all the points remain, and these already show quite good agreement with (4). Interpreting this trend, we conclude that, for a given value of l/η , in order for the moments to exhibit approximate scale similarity the value of r must be greater than or equal to a minimum critical value, which for the present data is about 36η .

The lack of scale similarity for $r/\eta < 36$ might have been anticipated, since scale similarity, if it occurs, is a feature of the inertial subrange. The peak of the dissipation spectrum occurs at a wavenumber k such that $k\eta = 0.2$, roughly; the corresponding wavelength is $2\pi/k \sim 30\eta$. Therefore $r/\eta \leq 36$ refers to scales which are strongly affected by viscous damping, and one would not expect scale similarity to hold at dissipative scales.

The present data and analysis of all available data thus strongly suggest that the theory of scale similarity furnishes an approximately valid description of the behaviour of the statistical properties of the breakdown coefficient for $r > 36\eta$ (or $l > 75\eta$), even though one of the underlying fundamental hypotheses of the theory, $p(q_{r,l}) = p(l/r)$, may not be closely satisfied by the data. This raises the important question of just how closely the data need to satisfy this hypothesis in order that the moments will be nearly scale similar, and how one can obtain

a relative measure of the degree to which it is satisfied. Re-examining the data for the probability densities shown in detail in I and partially summarized in the present figures 4 and 5, we note that for fixed l/r the rate of growth of the peak value of $p(q_{r,l})$ with increasing l/η , which is a measure of the deviation of $p(q_{r,l})$ from scale-similarity behaviour, is relatively slow, being only logarithmic in l/η . For $l/r = 2$, the peak value changes by a constant increment with each doubling of l/η . The percentage change in the probability density is therefore decreasing as l/η increases, increasing by only about 8% for a change in l/η from 580 to 1160. For larger values of l/r , the changes in $p(q_{r,l})$ with l/η are considerably smaller. From figure 7 of I, for $l/r = 4$, the peak value changes by only 4% as l/η increases from 580 to 1160. Although this easily measurable evolution follows a definite trend, we must ask whether or not the changes are large enough to cause the measured moments to exhibit significant deviations from the form specified in (4). For the smaller values of r , we have seen that they do cause significant deviations, while for the larger values we obtain the remarkably close scale similarity of the moments shown in figures 10 and 11.

We have also seen that measurements for the largest values of l/η exhibit very small changes in $p(q_{r,l})$. This implies that an extensive region of scale similarity might be found for values of l/η larger than those considered here (for which the maximum l is about 5 m), as first suggested by Kholmyansky (1973). This possibility is consistent with the trend, noted in I, that the rate of variation of the measured moments a_p with l/η for fixed l/r decreases as l/η increases. The present calculations have not been pursued to larger values of l/η because $l = 5$ m is already of the same order as the height of the probe above the ground, which corresponds roughly to the outer scale L referred to in §2.

Kholmyansky suggested that measurements should be obtained for considerably larger heights, where one might expect a broader interval of scale similarity. Such measurements could readily be obtained from a tall meteorological tower or from instrumented aircraft. No effect of the height of measurement z in the surface boundary layer was evident in the present measurements. As shown in figure 14 of I, the measured moments a_p for heights of 5.66 and 11.3 m are virtually identical. Detailed comparisons of probability densities, illustrated by the examples in figure 12, also showed no significant differences between the data obtained at these two heights. This suggests that for future measurements to investigate this point z should be at least an order of magnitude larger, say 100 m, which is within the capability of a number of existing towers.

4.4. The function $\alpha(s)$

The universal function $\alpha(s)$ given by (10) was calculated for several of the larger pairs of l and r , for which scale similarity may be most closely satisfied, and the results are shown in figure 13. The real and imaginary parts of α have the same general form as was found by Kholmyansky, but the present functions are somewhat larger in magnitude. The small amount of data considered suggests that α is approaching a universal form, as would be expected since α is calculated from the $p(q_{r,l})$ obtained for large scales. The difference between the present

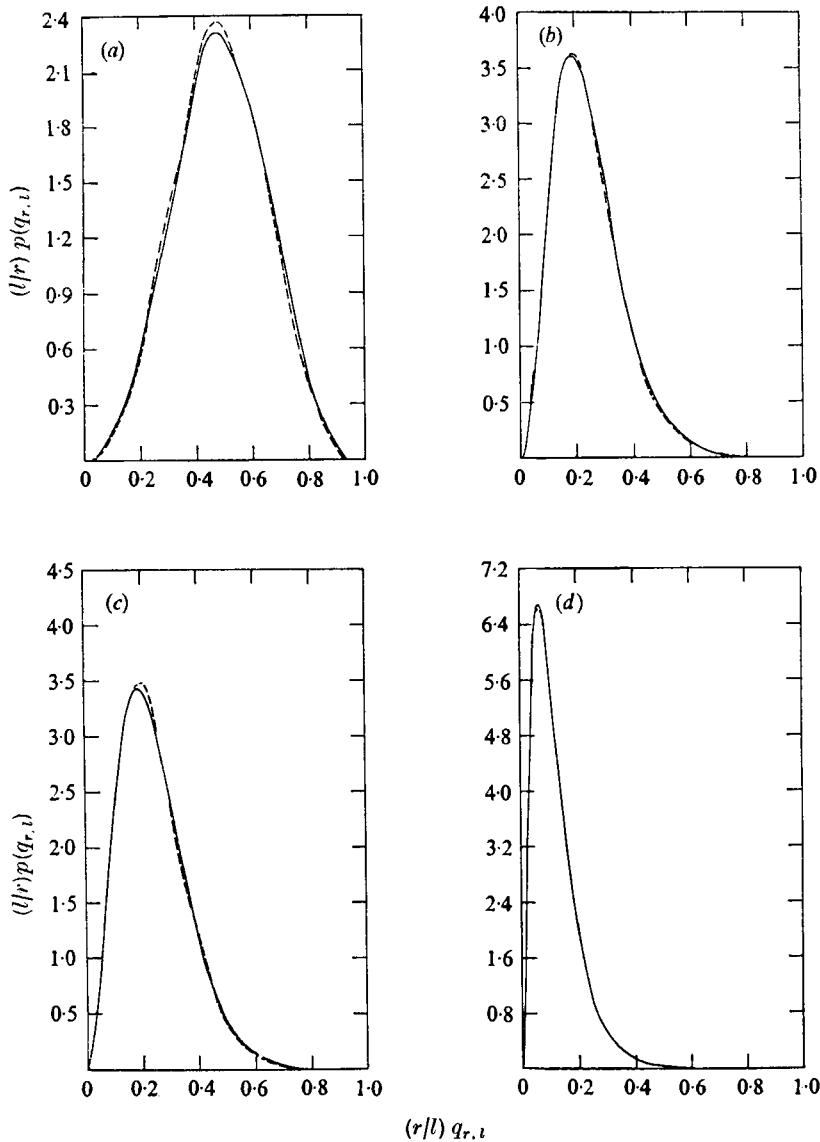


FIGURE 12. Comparison of $p(q_{r,l})$ for two different measurement heights in the atmospheric boundary layer. $h = 0$. (a) $l/r = 2$; —, $z = 5.66$ m, $l/\eta = 580$; ---, $z = 11.3$ m, $l/\eta = 630$. (b) $l/r = 4$; —, $z = 5.66$ m, $l/\eta = 4639$; ---, $z = 11.3$ m, $l/\eta = 5048$. (c) $l/r = 4$; —, $z = 5.66$ m, $l/\eta = 2320$; ---, $z = 11.3$ m, $l/\eta = 2522$. (d) $l/r = 8$; —, $z = 5.66$ m, $l/\eta = 4639$; ---, $z = 11.3$ m, $l/\eta = 5044$. $U = 4.47$ m s $^{-1}$ for $z = 11.3$ m.

functions and those obtained by Kholmyansky is caused by the observed differences in the measured $p(q_{r,l})$, and is a matter for further study.

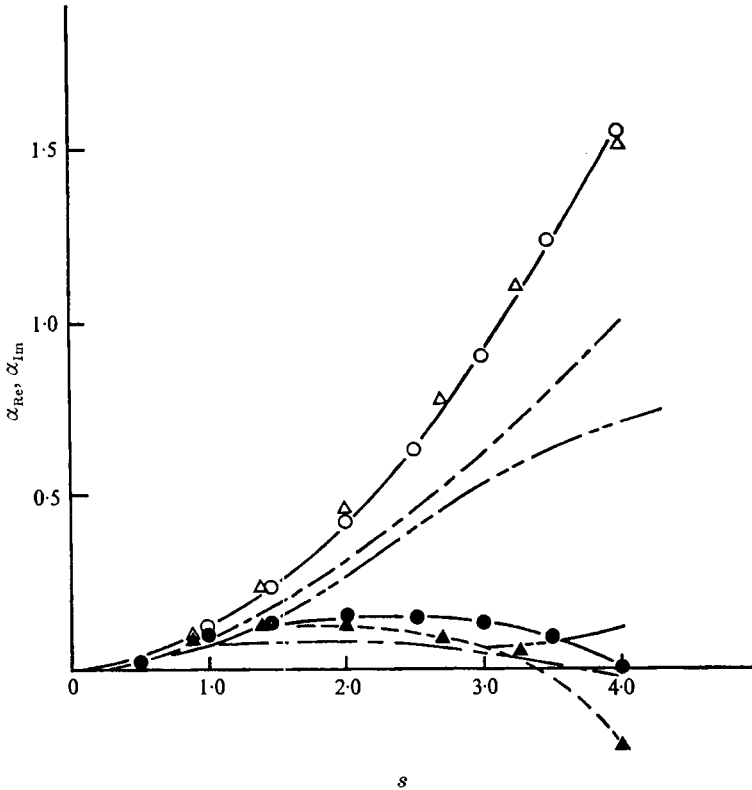


FIGURE 13. The function $\alpha(s)$ computed for large values of l . $h = 0$. Open symbols, real part of α ; closed symbols, imaginary part. Present data, ζ_2 , $z = 5.66$ m: \circ , $l = 4600\eta$, $r = 580\eta$; \triangle , $l = 2319\eta$, $r = 290\eta$. Kholmyansky, ζ_1 , $z = 13.5$ m: $-\cdot-$, $l = 12943\eta$, $r = 1618\eta$; $---$, $l = 25887\eta$, $r = 1618\eta$.

5. Conclusions

The new evidence presented here and the data of Kholmyansky require us to modify our previous conclusion expressed in I that the assumptions and predictions of the hypothesis of scale similarity do not adequately describe or predict the statistical characteristics of the breakdown coefficient $q_{r,l}$ of the square of the streamwise velocity derivative measured in an atmospheric boundary layer. There are systematic variations in the measured probability densities and consistent variations in the measured moments for the smaller values of l/η which show that the assumption that the probability density of the breakdown coefficient is a function only of the scale ratio is not generally satisfied. However, the rate of variation of $p(q_{r,l})$ decreases as l/η increases, becoming relatively unimportant for the largest values of l/η . Previous uncertainties about the degree of dependence of two sequential breakdown coefficients, which could not be resolved by the measurements made in I, have been resolved by making more definitive measurements of the associated characteristic functions. The computed characteristic functions satisfy the assumption of independence fairly well, a result that is consistent with the small measured values of the

cross-correlation coefficient reported in I. The data for the measured moments are consistent with the existence of a restricted range of scale similarity for the larger averaging lengths. If the data for the smaller lengths are excluded, i.e. only data for $r \geq 36\eta$ considered, then the measured moments are found to exhibit a behaviour very close to that predicted by the scale-similarity theory.

The measured moments and corresponding values of the parameters μ_p are in good agreement with those obtained by Kholmyansky. However, an unexplained difference of roughly a factor of two is found in the peak values of the probability densities for ζ_1 . The measured mean-square value of ζ_1 is always substantially larger than the corresponding mean-square value of ζ_2 . Comparison with the generalized Taylor hypothesis of Heskestad shows that $\mathcal{U}^{-1} \partial u / \partial t$ is not as good an approximation to $\partial u / \partial x$ as is $U^{-1} \partial u / \partial t$.

The present measured statistical properties of the breakdown coefficient are independent of the height above the ground at which the measurements were made. It would be useful to have measurements for much larger heights, where the relevant external scale of the turbulence is presumably larger, to see whether an even better agreement with the hypotheses and consequences of scale-similarity might be found over a larger range of scales.

The data used for the present measurements were gathered by the Boundary Layer Branch of the Air Force Cambridge Research Laboratories, Bedford, Massachusetts. We especially thank Dr J. C. Wyngaard of AFCRL for his loan of the analog tape. At USCD the work was supported by NSF grant GK-43643X, and by the Advanced Research Projects Agency of the Department of Defense, monitored by the U.S. Army Research Office, Durham, under contract DAHC04-72-C-0037.

REFERENCES

- GURVICH, A. S. & YAGLOM, A. M. 1967 Breakdown of eddies and probability distributions for small-scale turbulence. *Phys. Fluids Suppl.* **10**, S59.
- HESKESTAD, G. 1965 A generalized Taylor hypothesis with application for high Reynolds number turbulent shear flows. *J. Appl. Mech.* **32**, 735.
- KHOLMYANSKY, M. Z. 1972 Measurements of the turbulent microfluctuations of the wind velocity derivative in the atmospheric surface layer. *Izv. Akad. Nauk S.S.S.R., Phys. Atmos. Ocean*, **8**, 818.
- KHOLMYANSKY, M. Z. 1973 Measurements of the turbulence breakdown coefficient. *Izv. Akad. Nauk S.S.S.R., Phys. Atmos. Ocean*, **9**, 801.
- KOLMOGOROV, A. N. 1941 The local structure of turbulence in an incompressible fluid for very large Reynolds numbers. *Dokl. Akad. Nauk S.S.S.R.* **30**, 301.
- KOLMOGOROV, A. N. 1962 A refinement of previous hypotheses concerning the local structure of turbulence in a viscous incompressible fluid at high Reynolds number. *J. Fluid Mech.* **13**, 82.
- LANDAU, L. D. & LIFSHITZ, E. M. 1959 *Fluid Mechanics*. Pergamon.
- NOVIKOV, E. A. 1965 On higher-order correlations in a turbulent flow. *Izv. Akad. Nauk S.S.S.R., Ser. Geofiz.* **1**, 788.
- NOVIKOV, E. A. 1969 Similarity of scale for stochastic fields. *Dokl. Akad. Nauk S.S.S.R.*, **184**, no. 5.
- NOVIKOV, E. A. 1971 Intermittency and scale similarity in the structure of a turbulent flow. *Prikl. Math. Mech.* **35**, 266.

- NOVIKOV, E. A. & STEWART, R. W. 1964 Turbulent intermittency and the spectrum of fluctuations of energy dissipation. *Izv. Akad. Nauk S.S.S.R., Ser. Geophys.* no. 3.
- OBOUKHOV, A. M. 1941 On the distribution of energy in the spectrum of turbulent flow. *Dokl. Akad. Nauk S.S.S.R.* **32**, 19.
- OBOUKHOV, A. M. 1962 Some specific features of atmospheric turbulence. *J. Fluid Mech.* **13**, 77.
- RICHARDSON, L. F. 1920 The supply of energy to and from atmospheric eddies. *Proc. Roy. Soc. A* **97**, 354.
- VAN ATTA, C. W. & YEH, T. T. 1973 The structure of internal intermittency in turbulent flows at large Reynolds number: experiments on scale similarity. *J. Fluid Mech.* **59**, 537.
- WYNGAARD, J. C. & PAO, Y. H. 1972 Some measurements of the fine structure of large Reynolds number turbulence. In *Statistical Models and Turbulence. Lecture Notes in Physics*, vol. 12 (ed. M. Rosenblatt & C. Van Atta), p. 384. Springer.
- YAGLOM, A. M. 1966 On the influence of fluctuations in energy dissipation on the form of turbulence characteristics in the inertial range. *Dokl. Akad. Nauk S.S.S.R.* **166**, 49.